Charging and Aggregation of Positively Charged Colloidal Latex Particles in Presence of Multivalent Polycarboxylate Anions

By Amin Sadeghpour[#], Istvan Szilagyi, and Michal Borkovec[*]

Department of Inorganic and Analytical Chemistry, University of Geneva, Sciences II, 30, Quai Ernest-Ansermet, 1205 Geneva, Switzerland

Dedicated to Matthias Ballauff on the occasion of his 60th birthday

Colloidal stability and charging behavior of amidine latex particles in the presence of multivalent oligomers of acrylic acid was investigated by electrophoresis and light scattering. The data were interpreted quantitatively with the theory of Derjaguin, Landau, Verwey and Overbeek (DLVO) whereby the surface potentials were estimated from electrophoresis. Monomer leads to slow aggregation at low concentrations and to rapid aggregation at high concentrations, as characteristic for simple salts. The oligomers induce a charge reversal of the particles. Close to the isoelectric point (IEP) aggregation is rapid while the suspension becomes stable away from this point. At high oligomer concentrations, the aggregation becomes rapid again. The agreement between DLVO theory and experiment is good close to the IEP. At higher oligomer concentrations, the theory predicts larger stabilities than observed experimentally. While inter-particle forces seem to be well described by DLVO theory near the IEP, additional attractive non-DLVO forces are becoming relevant at higher concentrations.

1. Introduction

Effects of multivalent ions on colloidal stability were investigated from early on. An important motivation for these studies is the effectiveness of trivalent aluminum and iron ions to coagulate colloidal suspensions, and therefore such ions are widely exploited in water purification. The rational that multivalent ions should be effective coagulants derives from the Schulze–Hardy rule known for more than a century [1–4]. This rule states that the critical coagulation concentration c needed to destabilize a colloidal sus-

---

* Corresponding author. E-mail: michal.borkovec@unige.ch
\# *Present address*: Physical Chemistry, Karl-Franzens University, 28 Heinrichstrasse, 8010 Graz, Austria

pension scales as

$$c \propto z^{-6} \tag{1}$$

where z is the valence of the counterion. This relation was derived from the theory of Derjaguin, Landau, Verwey and Overbeek (DLVO) half a century ago [1,2]. This theory assumes that interaction forces between colloidal particles are dominated by attractive van der Waals and repulsive electrostatic double-layer forces. At high salt concentration, electrostatic interactions are screened and the aggregation process is fast. At low salt concentration, the balance between electrostatic and van der Waals interactions induces an energy barrier, which leads to slow aggregation. The theory predicts a sudden transition between fast and slow aggregation, and the corresponding salt concentration can be shown to scale according to Eq. (1). This theoretical success prompted further experimental studies, especially with multivalent metal cations [5–11]. While these experiments generally did confirm the validity of this rule, the inevitable hydrolysis of the metal cations complicates the picture substantially [6,12].

The renewed interest concerning interactions between particles induced by multivalent ions was spurred by the discovery that the commonly used Poisson–Boltzmann (PB) approach inherent to DLVO theory breaks down for highly charged surfaces and for higher valence [13–17]. Under these conditions, ion-ion correlations may cause charge reversal and induce attractive forces. These discoveries have spurred substantial research activity focusing on the influence of multivalent ions on interactions between surfaces. For example, multivalent ions were shown to modify the growth of polyelectrolyte multilayers [18] and to induce collapse of DNA [19,20], polysaccharides [21], or polyelectrolyte brushes [22,23].

However, little is known how ion-ion correlations affect colloidal stability in the presence of multivalent ions [24]. When these effects would become important, DLVO theory should break down. However, one knows that DLVO may describe colloidal stability for multivalent ions very well. A possible resolution of this dilemma is that ion-ion correlations are mainly important close to the surface, while the PB approach remains valid at larger distances. This point of view suggests, however, that the surface charge density entering DLVO theory is an effective charge density, which may be even different in sign from the charge of the bare surface. An alternative point of view is that multivalent ions adsorb on the surface in a specific fashion, which may also modify the surface charge that is relevant in the DLVO theory. These two eventually complementary point of views were recently contrasted in a review [25].

In the present article, we address this question by investigating the aggregation kinetics of positively charged colloidal particles in the presence of multivalent anions. Colloidal stability studies involving multivalent anions are rare, and we are only aware of the determination of the critical coagulation concentration of silver bromide particles in the presence of phosphotungstate anions [26]. However, these anions are strongly influenced by hydrolysis and precipitation reactions. The present article provides detailed aggregation rate measurements of cationic amidine latex particles in the presence of organic polycarboxylate anions. These measurements are compared with calculations based on DLVO theory whereby the surface potentials are estimated from electrophoresis. The relatively good agreement between experiment and theory suggests that DLVO

is indeed a good approximation, provided an appropriate charge density is being used. Some of the presented results were reported earlier to illustrate the transition between the aggregation behavior induced by oligomers and polyelectrolytes [27].

2. Experimental methods and data interpretation

2.1 Materials

Surfactant-free amidine functionalized polystyrene latex particles were purchased from International Dynamics Corporation (Portland, USA). The manufacturer determined a number averaged radius of 110 nm and a polydispersity characterized by a coefficient of variation of 4.3% by electron microscopy and a surface charge density of $+0.13\,C/m^2$ by conductivity. Dynamic light scattering experiments yield a hydrodynamic radius of 117 nm. The difference between the two reported radii is probably due to finite polydispersity of the sample. Prior to use, particles were purified by dialysis against Milli-Q water with a polyvinyl difluoride membrane with a molecular mass cutoff of 250 kg/mol until the conductivity of the surrounding solution was equal to the Milli-Q water used. The total particle concentration of the latex particles was determined by total carbon analysis (TOC, Shimadzu).

Glutaric acid and acetic acid were bought from Sigma-Aldrich (Steinheim, Germany). Glutaric acid has been filtered prior to use by 0.1 μm Millex syringe driven filter (Millipore, Ireland). Trimer, tetramer, and hexamer of acrylic acid with a polydispersity index < 1.2 were purchased from Polymer Source Incorporation (Montreal, Canada). The final concentration of the oligomers was determined by TOC. Their ionization constants were determined by potentiometric titrations in our laboratory [28–30]. They are summarized with few additional properties of the oligomers in Table 1.

Hydrochloric acid from Merck (Darmstadt, Germany) and CO_2-free potassium hydroxide from Mallinckrodt Baker (Deventer, Netherland) were used to adjust the solution pH and the ionic strength was set by potassium chloride (KCl) from Acros (Geel, Belgium). All experiments were carried out at pH 5.8 ± 0.1 and at a temperature of $25\,°C$.

2.2 Electrophoresis

Laser Doppler velocimetry was used to measure the electrophoretic mobility of the particles with a Zetasizer Nano ZS (Malvern Instruments, Worcestershire, UK). The electric field strength was around 4 kV/m. The oligomer concentrations were adjusted by mixing comparable volumes of latex suspensions and pre-equilibrated oligomer solutions. Electrophoretic mobilities were recorded after 2–3 h equilibration time. Samples were prepared by mixing water with the appropriate volume of electrolyte solution to reach the desired ionic strength. Subsequently, particles were added from a concentrated stock solution to achieve a final particle concentration of 11 mg/L. The oligomer concentrations were adjusted by mixing comparable volumes of latex suspensions and pre-equilibrated oligomer solutions in the appropriate concentration range. The elec-

Table 1. Properties of acrylic acid oligomers and of amidine latex particles in their presence.

Name	Symbol	Ionization constants	Ionization degree	IEP (mg/L)[c]	Partitioning (%)[c,d]
Acetic acid	C1	4.76[a]	0.92	1.1×10^5	> 90
Glutaric acid	C2	4.35, 5.42[a]	0.85	2.3×10^3	> 90
1-(2-methylbutyl)pentan-1,3,5-tricarboxylic acid	C3	4.15, 4.96, 6.09[b]	0.78	6.5	> 83
1-(2-methylbutyl)heptane-1,3,5,7-tetracarboxylic acid	C4	4.46, 4.51, 5.51, 6.67[b]	0.74	0.87	82
1-(2-methylbutyl)undecan-1,3,5,7,9,11-hexacarboxylic acid	C6	3.83, 5.09, 4.91, 6.68, 5.90, 7.85[b]	0.66	0.08	33

[a] Extrapolated to vanishing ionic strength and at 25 °C from [43]. [b] Measured by potentiometric titration at different ionic strengths in KCl electrolyte and extrapolated to vanishing ionic strength and at 25 °C. [c] Measured by electrophoresis in 1 mM KCl and at pH 5.8. [d] At a particle concentration of 11 mg/L and at IEP.

trophoretic mobility u was converted to surface potentials with the Henry equation

$$u = f(\kappa r) \frac{\varepsilon_0 \varepsilon}{\eta} \zeta \tag{2}$$

where ε and η are the dielectric constant and viscosity of water, respectively, ε_0 is the dielectric permittivity of vacuum, ζ is the electric surface potential and $f(x)$ is the Henry function [31]. The arguments of this function involve the particle radius r and the inverse Debye length κ, which is defined by

$$\kappa^2 = \frac{2\beta e^2 N_A}{\varepsilon_0 \varepsilon} I \tag{3}$$

where $\beta = 1/k_B T$ is the inverse thermal energy, e the elementary charge, N_A Avogadro's number, and I is the ionic strength. The latter is given by the sum over all ions present

$$I = \frac{1}{2} \sum_i z_i^2 c_i \tag{4}$$

where c_i and z_i is the molar concentration and valence of the ion of type i, respectively.

The extent of oligomer partitioning between dissolved and adsorbed state was estimated by comparing the respective total concentrations $c_{t,1}$ and $c_{t,2}$ needed to reach the IEP at two different particle mass concentrations $c_{p,1}$ and $c_{p,2}$. The two particle concentrations were chosen around 4 mg/L and 400 mg/L. We assume equilibrium conditions and that the electrophoretic mobility if only a function of the total adsorbed amount Γ, which in itself is only a function of the solution concentration, one has [32]

$$\Gamma = \frac{c_{t,1} - c_d}{c_{p,1}} = \frac{c_{t,2} - c_d}{c_{p,2}} \tag{5}$$

where c_d is the solution concentration of the oligomers. From Eq. (5) one obtains the solution concentration and subsequently the dissolved fraction of the oligomer in solution from $1 - \Gamma c_{p,1}/c_{t,1}$. The partitioning at 11 mg/L was obtained by noting that the adsorbed amount Γ is independent of particle concentration.

2.3 Suspension stability by light scattering

Time-resolved light scattering experiments were used to study particle aggregation. The samples were prepared in a similar fashion as for the mobility measurements in borosilicate glass cuvettes. Absolute rate constant measurements were carried out on a multi-angle light scattering instrument (ALV/CGS-8, Langen, Germany) with a solid state laser operating at a wavelength of 532 nm (Verdi V2, Coherent, Inc.) and 8 fiber-optic photomultiplier detectors. Stability ratios were measured on a compact goniometer (ALV/CGS-3, Langen, Germany) with a He-Ne laser of 633 nm wavelength as a light source and an avalanche photodiode as a detector at a scattering angle of 90°. In both cases, each correlation function was accumulated for 20 seconds. The apparent hydrodynamic radius was obtained from a second order cumulant fit. The time-evolution of this quantity was monitored through 70–500 consecutive measurements.

The absolute aggregation rate coefficient k was calculated by comparing time dependence of the static light scattering intensity $I(q, t)$ and of the apparent hydrodynamic radius $r_h(q, t)$. In the early stages of the aggregation process, the initial rate of the static intensity yields the static signal S, which is given by [33,34]

$$S = \frac{1}{I(q, 0)} \cdot \frac{dI(q, t)}{dt}\bigg|_{t \to 0} = kn_0 \left(\frac{I_2(q)}{2I_1(q)} - 1 \right) \tag{6}$$

where n_0 the initial particle number concentration, q is the magnitude of the scattering vector, and $I_1(q)$ and $I_2(q)$ are the scattering intensities of the monomers and dimers, respectively. The initial rate of change of the hydrodynamic radius yields the dynamic signal D, which is given by [33,34]

$$D = \frac{1}{r_h(q, 0)} \cdot \frac{dr_h(q, t)}{dt}\bigg|_{t \to 0} = \left(1 - \frac{1}{\alpha} \right) \frac{I_2(q)}{2I_1(q)} kn_0 \tag{7}$$

where $\alpha = r_{h,2}/r_{h,1}$ is the ratio of the hydrodynamic radii $r_{h,1}$ and $r_{h,2}$ which refer to the monomer and the dimer, respectively. Combining Eqs. (6) and (7) one finds that the initial rates of change of these two quantities obey a linear relationship, namely

$$S = \left(1 - \frac{1}{\alpha} \right)^{-1} D - kn_0 \tag{8}$$

Therefore, one can obtain the absolute aggregation rate constant from time-resolved simultaneous static and dynamic light scattering measurements without making any assumptions on the optical and hydrodynamic properties of the particles. Such experiments were carried out in 0.5 M KCl electrolyte at pH 4.0 and a particle concentration of 0.5 mg/L. These two quantities S and D indeed fall on a straight line as shown
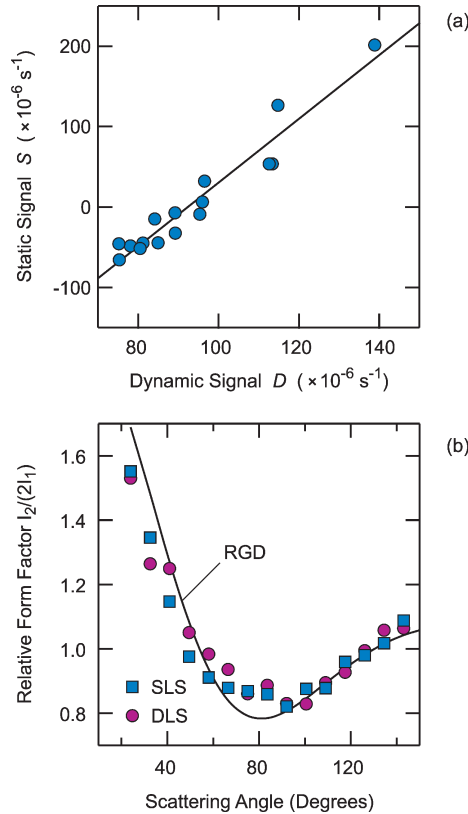
Fig. 1. Determination of the absolute aggregation rate constant by SSDLS in 0.5 M KCl electrolyte solution and pH 4.0 at a particle concentration of 0.5 mg/L. (a) Scatter plot of the static signal *vs.* the dynamic signal. (b) The relative form factor as a function of the scattering angle obtained from static light scattering (SLS) and dynamic light scattering (DLS) and compared with the theory of Rayleigh, Gans, and Debye (RGD).

in Fig. 1a. The best fit of these data points yield an aggregation rate constant of 4.4×10^{-18} m^3/s and a ratio of the hydrodynamic radii $\alpha \simeq 1.34$. This value compares reasonably well with the theoretical value of 1.38 based on low Reynolds number hydrodamics [33,34]. Once these parameters are known, the relative form factor can be evaluated from the angle-resolved measurements and compared to the expression given by the theory by Rayleigh, Gans, and Debye (RGD)

$$\frac{I_2(q)}{2I_1(q)} = 1 + \frac{\sin(2qr)}{2qr} \qquad (9)$$

This expression is shown together with the relative form factors obtained experimentally from static and dynamic light scattering in Fig. 1b. One observes that in the present case the RGD approximation is relatively good. In the following, the aggregation rate

constants are expressed as the stability ratio

$$W = \frac{k_{\text{fast}}}{k} \tag{10}$$

where k_{fast} is the fast aggregation rate coefficient in excess salt. The stability ratios were determined from rate of change of hydrodynamic radius measured by dynamic light scattering at a single angle as given by Eq. (7). For the particles studied here, fast aggregation is reached above the critical coagulation concentration (CCC) situated around 0.13 M. Further experiments demonstrated that k_{fast} is independent of pH within experimental error.

2.4 DLVO calculations

The stability ratio was calculated from aggregation rate coefficient that is obtained from the steady-state solution of the forced diffusion equation [3,35]

$$k = \frac{4}{3\beta\eta r} \left[\int_0^\infty \frac{B(h/r)}{(2r+h)^2} \exp[\beta V(h)] \mathrm{d}h \right]^{-1} \tag{11}$$

where h is the separation between the particles, $V(h)$ the interaction potential energy, and the hydrodynamic resistance function $B(x)$ that is well approximated by

$$B(x) = \frac{6x^2 + 13x + 2}{6x^2 + 4x} \tag{12}$$

The DLVO theory expresses the total interaction energy as

$$V(h) = V_{\text{vdW}}(h) + V_{\text{dl}}(h) \tag{13}$$

where $V_{\text{vdW}}(h)$ is the van der Waals and $V_{\text{dl}}(h)$ the electrostatic double layer energy. Since the particles are large compared to the range of the interaction potential, the Derjaguin approximation is used throughout. The van der Waals interaction energy can be evaluated from [3]

$$V_{\text{vdW}}(h) = -\frac{Ar}{12h} \tag{14}$$

where A is the Hamaker constant. Debye-Hückel theory was used to calculate repulsive electrostatic interaction energies at constant potential (CP) and constant charge (CC) boundary conditions [36,37]. The ionic strength of the solution was estimated from Eq. (4) by calculating the relative concentrations of the various species resulting from the partial dissociation of the oligomers based on the known ionization constants extrapolated to vanishing ionic strength (Table 1) and by applying the Davies expression to evaluate the activity coefficients. The electrical surface potential was obtained by interpolating the electrophoresis data and converting them to surface potential with Eq. (2). The calculations were checked with the Poisson–Boltzmann approximation and the results were very similar.
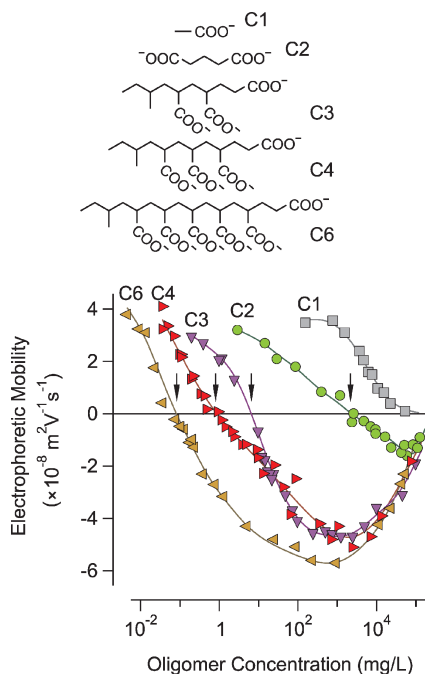
Fig. 2. Fully ionized acrylic acid oligomers used (top) and the electrophoretic mobility of amidine latex particles *vs.* the oligomer concentration at pH 5.8 and an added KCl concentration of 1 mM (bottom). The particle concentration is 11 mg/L. Solid lines are interpolations by an empirical fitting function. Arrows indicate the IEPs.

3. Results and discussion

Charging and stability of positively charged amidine latex particles are studied in the presence of acrylic acid oligomers of different valence, namely for monomers (C1), dimers (C2), trimers (C3), tetramers (C4) and hexamers (C6). Some of the relevant properties of the oligomers are summarized in Table 1. Stability ratios measured by dynamic light scattering can be rationalized with calculations based on DLVO theory, whereby the electric surface potentials are estimated from electrophoresis. Overcharging and screening phenomena dictate the stability behavior in these systems.

3.1 Charging behavior

Electrophoretic mobility of the positively charged latex particles is shown in Fig. 2 *vs.* the oligomer concentration at pH 5.8 and with 1 mM KCl electrolyte added. Oligomers of higher valence induce overcharging. While increasing concentration of C1 leads to a continuous decrease of the electrophoretic mobility, C2 already induces a charge reversal at the isoelectric point (IEP) and subsequent overcharging. With increasing valence of the oligomers, the IEP shifts towards lower oligomer concentrations. The oligomers of higher valence, namely C3, C4, and C6 lead to such a pronounced over-
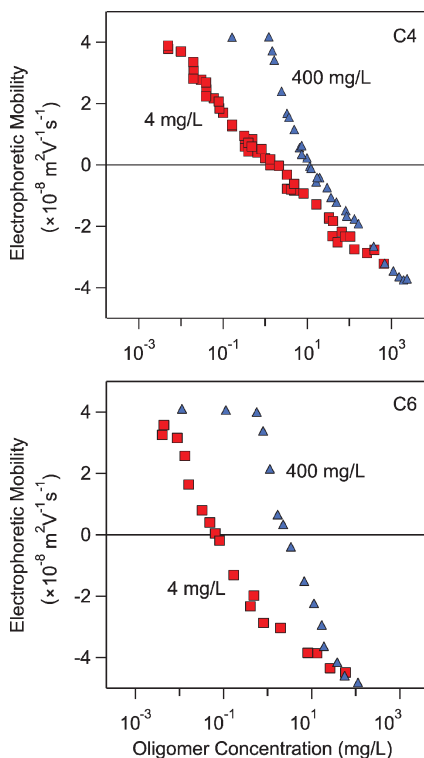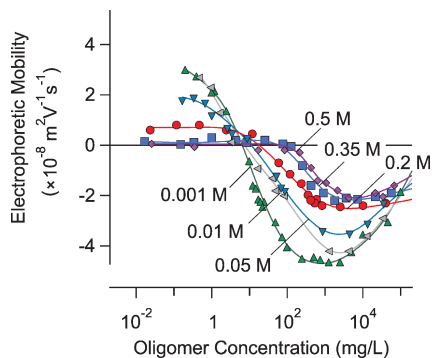
Fig. 3. The electrophoretic mobility of amidine latex particles in the presence of acrylic acid oligomer C4 (top) and C6 (bottom) at pH 5.8 and an added KCl concentration of 1 mM for two different particle concentrations. The shift between these curves indicates that partitioning between the adsorbed and dissolved state exists.

charging, that the mobility passes through a minimum, and increases again at higher concentrations.

This behavior can be interpreted as follows. The oligomers of higher valence adsorb strongly on the latex particle surface and reverse the particle charge from positive to negative. Since the affinity of the oligomers to the oppositely charged particle surface increases with increasing valence, one observes that the IEP shifts towards lower concentrations. With increasing concentrations, however, the oligomers partition progressively into the solution. At higher concentrations, they are principally in the dissolved state, and only a small amount remains adsorbed. At very high concentrations, the highly charged dissolved oligomers represent the dominant contribution to the ionic strength, and substantially screen the surface charge through their counterions. This screening leads to a decrease in the magnitude of the surface potential and to a decrease in the electrophoretic mobility. C1 hardly adsorbs and therefore the mobility is reduced only through screening.

Even at IEP, the oligomers are partitioned such that they are principally dissolved in solution. This point was verified by studying the electrophoretic mobility as a function

Fig. 4. Electrophoretic mobility of amidine latex particles *vs.* the concentration of the acrylic acid oligomer C3 for different added KCl concentration and pH 5.8. The particle concentration is 11 mg/L. Solid lines are interpolations by an empirical fitting function.

of oligomer dose at different particle concentrations. Typical results are shown in Fig. 3. One observes a substantial shift in the electrophoretic mobility for the different concentrations. This shift indicates a partitioning between dissolved and adsorbed species [32]. Assuming that the same amount is adsorbed at IEP, one can obtain an estimate of the degree of partitioning from the shift of IEP by applying Eq. (5). The results are summarized in Table 1. The oligomers up to C4 partition into the solution more than 80%. Adsorption becomes more important for C6, but about 30% remains still in solution.

The effect of added monovalent salt KCl on the electrophoretic mobility is shown in Fig. 4. At low salt levels, the overcharging process determines the mobility at low C3 concentrations, while at higher concentrations screening sets in. The influence of added salt becomes important at relatively high concentrations, where added oligomers also contribute to screening and reduce the mobility accordingly. Furthermore, the position of the IEP shifts towards higher oligomer concentrations, indicating that the salt anions compete with the oligomers for adsorption sites.

3.2 Colloidal stability

Stability ratios of the amidine latex particles in the presence of acrylic acid oligomers of different valence are shown in Fig. 5 at pH 5.8 and added concentration of 1 mM KCl. For C1, the particles are stable at low concentrations, while they become unstable at high concentration. For higher valence, two regimes of fast aggregation emerge. In the first regime, which occurs at low concentration, the system goes from slow to fast and back to slow aggregation in a narrow concentration range. In the second regime, which occurs at high concentrations, the aggregation accelerates as the concentration is being increased. These two regimes are clearly developed for C3 and higher. The transition between these regimes occurs at C2, whereby the first fast aggregation regime extends over relatively wide concentration range, while the intermediate stabilization only occurs in a rather narrow window.

Comparison with electrophoretic data reveals that the first fast aggregation regime coincides exactly with the IEP, suggesting that the charge reversal and subsequent over-
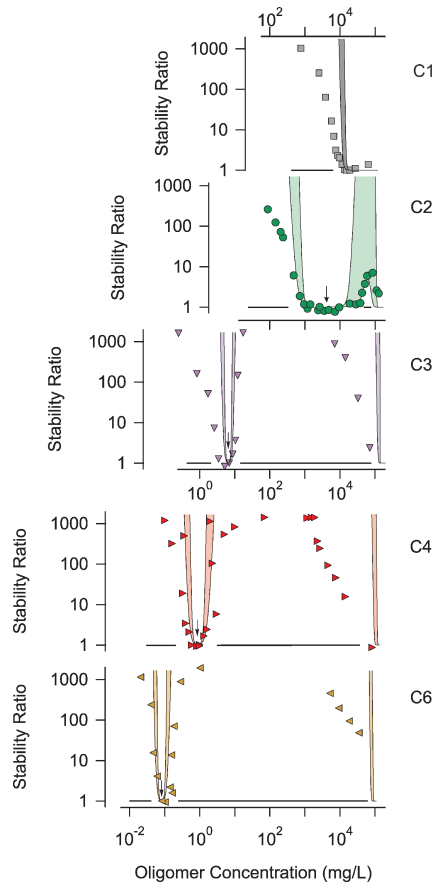
Fig. 5. Stability ratio of amidine latex particles in the presence of different acrylic acid oligomers at pH 5.8 and an added KCl concentration of 1 mM. The shaded regions are DLVO theory predictions with borders given by constant charge (CC) and constant potential (CP) boundary conditions.

charging are responsible for this behavior. The second fast aggregation regime occurs at much higher concentrations and originates from screening by monovalent cations.

The observed behavior can be summarized in a stability map shown in upper part of Fig. 6. This map shows the oligomer concentration on the ordinate and the valence on the abscissa, while the points corresponds to the CCCs. The narrow river-like instability region corresponds to the charge reversal at IEP. The delta-like instable region reflects screening with oligomers of low valence and high concentrations. The coast-like region at high concentrations is due to destabilization of the overcharged particles by monovalent cations. The solid line indicates the expected dependence on the Schulze–Hardy rule given by Eq. (1). The instability region around IEP follows this dependence relatively well at higher valence.

Added monovalent salt (KCl) has a substantial effect on the intermediate stability regime. These trends are illustrated in more detail for C3 in Fig. 7. At low salt concen-
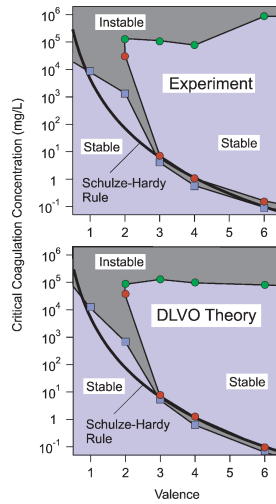
Fig. 6. Stability map showing the oligomer concentration *vs.* the oligomer valence observed experimentally (top) and calculated with DLVO theory (bottom) at pH 5.8 and for an added KCl concentration of 1 mM. The solid line indicates the dependence expected according to the Schulze–Hardy rule.
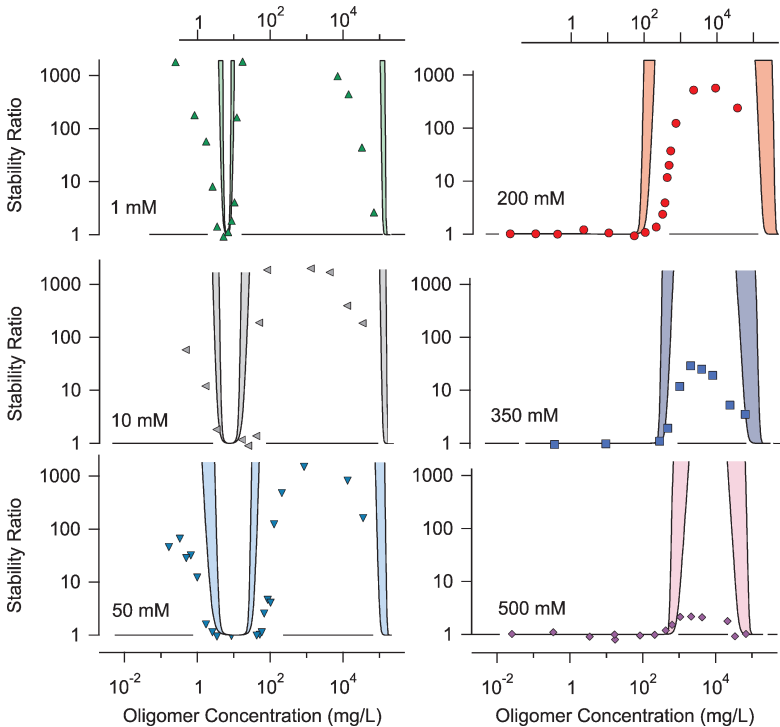
Fig. 7. Colloidal stability of the amidine latex particles in presence of acrylic acid trimer C3 at pH 5.8 and for different added KCl concentrations. The lines are predicted by DLVO theory at boundary conditions of constant charge (CC) and constant potential (CP).
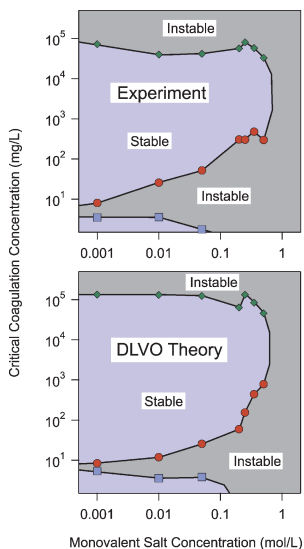
Fig. 8. Stability map for C3 showing the oligomer concentration *vs.* the concentration of added KCl observed experimentally (top) and calculated with DLVO theory (bottom) at pH 5.8.

tration, the two fast aggregation regimes are separated by a wide region of stability. As the salt concentration increases, the region of stability shrinks and the values of the intermediate maximum in the stability ratio diminish. Aggregation becomes rapid for all oligomer concentrations at salt concentrations above 1 M. The added salt influences the stability in two ways. First, it increases the ionic strength and thus contributes to screening of the electrostatic interactions. Second, it competes with the adsorbed oligomers and thereby reduces the surface charge.

The corresponding stability map is shown in the upper part of Fig. 8, whereby the abscissa represents the KCl concentration added. The narrow instability region at low concentration and salt corresponds to the charge reversal at IEP. The wide stability region corresponds to the overcharged particles, which become instable due to screening at high oligomer or salt concentration.

3.3 Predictions of DLVO theory

The observed trends in the colloidal stability can be predicted with DLVO theory relatively well. Thereby, the electric surface potentials are estimated by interpolating the electrophoretic mobility with an empirical fitting function (solid lines in Figs. 2 and 4) and converted with Henry's theory to surface potentials. These potentials are used in DLVO calculations invoking the Debye-Hückel approximation for constant charge (CC) and constant potential (CP) boundary conditions. The ionic strength was estimated by assuming that the total concentration of the oligomers is equal to their concentration is solution, and the partial ionization of the weak acid oligomers was considered by calculation the distribution of the differently charged species from the respective ionization constants. Attractive van der Waals forces were modeled with

a Hamaker constant of 2×10^{-21} J, which was adjusted to obtain the best agreement with experimental data. Note that this value is somewhat lower than the available theoretical estimate of the Hamaker constant of 9×10^{-21} J [38]. The predictions of DLVO theory are shown in Figs. 5 and 7. Thereby, the shaded region represents the regime between CC and CP boundary conditions. For all predictions shown in the figures, the electric potentials remain below 25 mV in magnitude. The magnitudes of the potentials may become higher in between, but for these conditions DLVO theory predicts stability ratios, which are out of the scale represented in the figures. This assumption of full partitioning into solution is not entirely satisfied for C6, and therefore the calculations were repeated by assuming that only 30% of the oligomers are dissolved. These results are indistinguishable on the scale in Fig. 5 to the ones shown.

Comparing DLVO predictions with the experimental data in Fig. 5 one observes that the width of the fast aggregation regime around the IEP is predicted rather well. On the other hand, the DLVO theory predicts a more sudden onset of the fast aggregation regime at high concentrations than observed experimentally. In this regime, the overcharged particles are negative, and they are destabilized by the monovalent cations present. Under these circumstances, DLVO theory is known to seriously overestimate the stability in such systems, since the barrier in the interaction potential is located at distances below one nanometer [24,39,40]. At these distances, small scale surface charge heterogeneities become important and they are probably responsible for the observed discrepancies. Ion-ion correlations effects might be another possible explanation of these deviations.

A stability map has been obtained from DLVO calculations and the result is shown in the bottom part of Fig. 6. Thereby, the CP boundary conditions were used, but CC conditions gave similar results. The calculated map agrees well with the experimental one. However, an important disagreement occurs at higher concentrations and at higher valence. In this regime, the overcharged particles are screened by monovalent cations, and as discussed above, the DLVO theory is known to perform in this situation poorly.

The reduction in the stability by addition of monovalent salt is modeled less accurately, as can be seen in Figs. 7 and 8. While the boundaries of the stabilization are predicted rather well, the DLVO theory overestimates the stability in the intermediate region. This overestimation is not surprising since the system is destabilized by monovalent counterions, and such disagreements are typical for DLVO theory in excess of monovalent salt. The corresponding stability map shown in the bottom part of Fig. 8 is in good agreement with the experimental one, but disagreement is observed at high salt concentrations. This disagreement is again related to the tendency of DLVO to overestimate the stability in the presence of monovalent counterions.

4. Conclusion

The effect of multivalent acrylic acid oligomers on the stability of amidine latex particles was investigated experimentally by electrophoresis and time-resolved light scattering. Highly charged oligomers induce a charge reversal at IEP. Close to the IEP, the aggregation is rapid, while the suspension becomes stable away from this point. At high oligomer concentrations, the aggregation becomes rapid again. The monomer does not

lead to a charge reversal, but induces slow aggregation at low concentrations, while the aggregation becomes rapid at high concentrations. This situation is characteristic for simple salts. This behavior can be well rationalized by DLVO theory, provided the surface potentials are estimated from electrophoresis. The agreement between theory and experiment is very good around the IEP. At higher concentrations, the theory predicts the stability to be higher than observed experimentally. One can conclude that interparticle forces are well described by DLVO theory close to the IEP, while additional attractive non-DLVO forces become relevant at higher concentrations. These forces could originate from discreteness of charge or ion-ion correlation effects. The latter effects could be equally important in inducing the overcharging, even though overcharging could also be induced by dispersion or hydrophobic forces. The overcharging observed for higher oligomers strongly resembles the influence on colloid stability by oppositely charged polyelectrolytes [27,41,42]. The main difference to the latter case is that polyelectrolytes adsorb quantitatively near the IEP.

Acknowledgement

References

1. B. Derjaguin and L. D. Landau, Acta Phys. Chim. **14** (1941) 633.
2. E. J. W. Verwey and J. T. G. Overbeek, *Theory of Stability of Lyophobic Colloids*, Elsevier, Amsterdam (1948).
3. W. B. Russel, D. A. Saville, and W. R. Schowalter, *Colloidal Dispersions*, Cambridge University Press, Cambridge (1989).
4. M. Elimelech, J. Gregory, X. Jia, and R. A. Williams, *Particle Deposition and Aggregation: Measurement, Modeling, and Simulation*, Butterworth-Heinemann Ltd., Oxford (1995).
5. B. Tezak, E. Matijevic, and K. F. Schulz, J. Phys. Chem. **59** (1955) 769.
6. E. Matijevic, D. Broadhurst, and M. Kerker, J. Phys. Chem. **63** (1959) 1552.
7. I. M. Metcalfe and T. W. Healy, Faraday Discuss. **10** (1990) 335.
8. D. Grolimund, M. Elimelech, and M. Borkovec, Colloids Surf. A **191** (2001) 179.
9. M. Sano, J. Okamura, and S. Shinkai, Langmuir **17** (2001) 7172.
10. K. L. Chen, S. E. Mylon, and M. Elimelech, Langmuir **23** (2007) 5920.
11. P. Yi and K. L. Chen, Langmuir **27** (2011) 3588.
12. R. O. James and T. W. Healy, J. Colloid Interface Sci. **40** (1972) 53.
13. L. Guldbrand, B. Jonsson, H. Wennerstrom, and P. Linse, J. Chem. Phys. **80** (1984) 2221.
14. R. Kjellander and S. Marcelja, Chem. Phys. Lett. **112** (1984) 49.
15. R. Kjellander and H. Greberg, J. Electroanal. Chem. **450** (1998) 233.
16. R. Kjellander, T. Akesson, B. Jonsson, and S. Marcelja, J. Chem. Phys. **97** (1992) 1424.
17. A. Y. Grosberg, T. T. Nguyen, and B. I. Shklovskii, Rev. Mod. Phys. **74** (2002) 329.
18. V. Ball, E. Hubsch, R. Schweiss, J. C. Voegel, P. Schaaf, and W. Knoll, Langmuir **21** (2005) 8526.
19. M. O. Khan and B. Jonsson, Biopolymers **49** (1999) 121.
20. M. O. Khan, S. M. Mel'nikov, and B. Jonsson, Macromolecules **32** (1999) 8836.
21. O. G. Jones, S. Handschin, J. Adamcik, L. Harnau, S. Bolisetty, and R. Mezzenga, Biomacromolecules **12** (2011) 3056.

22. Y. Mei, K. Lauterbach, M. Hoffmann, O. V. Borisov, M. Ballauff, and A. Jusufi, Phys. Rev. Lett. **97** (2006) 158301.
23. C. Schneider, A. Jusufi, R. Farina, F. Li, P. Pincus, M. Tirrell, and M. Ballauff, Langmuir **24** (2008) 10612.
24. C. Schneider, M. Hanisch, B. Wedel, A. Jusufi, and M. Ballauff, J. Colloid Interface Sci. **358** (2011) 62.
25. J. Lyklema, Colloid Surf. A **291** (2006) 3.
26. E. Matijevic and M. Kerker, J. Phys. Chem. **62** (1958) 1271.
27. I. Szilagyi, A. Sadeghpour, and M. Borkovec, Langmuir **28** (2012) 6211.
28. A. Sadeghpour, A. Vaccaro, S. Rentsch, and M. Borkovec, Polymer **50** (2009) 3950.
29. M. Borkovec, B. Jonsson, and G. J. M. Koper, Colloid Surface Sci. **16** (2001) 99.
30. M. Borkovec and G. J. M. Koper, J. Phys. Chem. **98** (1994) 6038.
31. S. R. Deshiikan and K. D. Papadopoulos, Colloid Polym. Sci. **276** (1998) 117.
32. A. Mezei and R. Meszaros, Langmuir **22** (2006) 7148.
33. H. Holthoff, S. U. Egelhaaf, M. Borkovec, P. Schurtenberger, and H. Sticher, Langmuir **12** (1996) 5541.
34. W. Lin, M. Kobayashi, M. Skarba, C. Mu, P. Galletto, and M. Borkovec, Langmuir **22** (2006) 1038.
35. M. Kobayashi, M. Skarba, P. Galletto, D. Cakara, and M. Borkovec, J. Colloid Interface Sci. **292** (2005) 139.
36. S. L. Carnie and D. Y. C. Chan, J. Colloid Interface Sci. **161** (1993) 260.
37. M. Borkovec and S. H. Behrens, J. Phys. Chem. B **112** (2008) 10795.
38. M. A. Bevan and D. C. Prieve, Langmuir **15** (1999) 7925.
39. S. H. Behrens, M. Borkovec, and P. Schurtenberger, Langmuir **14** (1998) 1951.
40. L. Ehrl, Z. Jia, H. Wu, M. Lattuada, M. Soos, and M. Morbidelli, Langmuir **25** (2009) 2696.
41. A. Sadeghpour, E. Seyrek, I. Szilagyi, J. Hierrezuelo, and M. Borkovec, Langmuir **27** (2011) 9270.
42. M. Borkovec and G. Papastavrou, Curr. Opin. Colloid Interface Sci. **13** (2008) 429.
43. A. E. Martell, R. M. Smith, and R. J. Motekaitis, Critically Selected Stability Constants of Metal Complexes: Version 8.0, National Insitutue of Standards and Technology, Gainesburg, 2004.